

Syntheses, Structures, and Theoretical Studies of New Ternary Antimonides β -RECoSb₃ (RE = La–Nd, Sm)

Wei-Zhao Cai,^[a,b] Li-Ming Wu,^[a] Long-Hua Li,^[a,b] and Ling Chen*^[a,c]

Keywords: Transition metals / Rare earth metal compounds / Cobalt / Antimon / Electronic structure / Calculations / Tight-bonding linear muffin-tin orbital method

Five new intermetallic ternary cobalt antimonides β -RECoSb₃ have been prepared by solid state reactions and characterized by single-crystal X-ray diffraction. The title compounds crystallize in β -RENiSb₃-type structure, *Pbcm* (No.57), *Z* = 8, with *a* = 12.985(4)–12.5530(13) Å, *b* = 6.1603(18)–6.1043(4) Å, *c* = 12.166(4)–12.0267(12) Å for RE = La, Ce, Pr, Nd, and Sm. Their structures feature the anionic Sb square nets and CoSb₆ octahedron layers that are separated by RE³⁺ cations along the *a* axis. The structural relationship among parent-type (RECrSb₃), α -type (RENiSb₃), and β -type (RECoSb₃) has been presented. The electronic

band structure of β -LaCoSb₃ has been calculated with the aid of the tight-bonding linear muffin-tin orbital (TB-LMTO) method and the results suggest that the three types of RE₂Sb₃ are metallic in both *b* and *c* directions and the electrical conductivities along the *a* direction are relatively weak. The magnetic calculations indicated that the rare-earth atoms would be the only source for the magnetic properties. Therefore, β -type Co analogues should be magnetically identical to the corresponding Ni members.

(© Wiley-VCH Verlag GmbH & Co. KGaA, 69451 Weinheim, Germany, 2009)

Introduction

Rare-earth transition-metal antimonides have been studied continuously because of their structural diversity, unique bonding interactions, and various interesting physical properties.^[1–3] The main structural motif of the layered RE₂Sb₃ family (RE = La–Nd, Sm, Gd–Dy, Yb; T = V, Cr, and Pd) are the condensed TSb₆ octahedron layers and the square Sb nets that are separated by the RE³⁺ cations along the stacking direction.^[4–13] Such anisotropic structure leads to the anisotropic electrical conductivity of LaCrSb₃, and the ferromagnetic behavior corresponds to the existence of an intermediate between Cr³⁺ and Cr⁴⁺.^[7] For other RECrSb₃ members (RE = Ce–Nd, Sm), the transition metal Cr influences the magnetic behaviors by coupling with RE at about 10 K.^[8,14–16] However, the V analogs (RE = La–Nd, Sm) show no 3*d* moment, and rare-earth cations are the sole magnetic source.^[4,6,14]

The RENiSb₃ exhibits interesting α - and β -type polymorphism. The α -RENiSb₃ (RE = Ce, Pr, Nd, Sm) differs from RECrSb₃ (named “parent type” hereafter) by a tripled *c* parameter, but similar TSb₆ layer and Sb net. The electrical conductivity perpendicular to the stacking direction is metallic. Unlike the parent structure type, the transition metal in the α -type has no significant contributions on the magnetic properties, and this series of compounds only show effective moments of free RE³⁺ ions.^[17,18]

The β -RENiSb₃ (RE = La, Ce) differs from the parent type by a doubled *c* parameter. And β -type compounds are also metallic perpendicular to the stacking direction; the Ce member shows ferromagnetic ordering of Ce³⁺ free ion only.^[19] The disordered analogs of RENi(Sn,Sb)₃ (RE = Pr, Nd, Sm, Gd, and Tb) confirm that the RE³⁺ ions are the sole source of the magnetic properties.^[20] However, the transition metal Ni has no contribution to the magnetic property in both α - and β -type RENiSb₃.^[17–19] The replacement of Ni by Co would provide a new opportunity to look for structural and magnetic correlations.

The known RE/Co/Sb compounds are RE₅CoSb₂ (RE = Gd, Tb, Dy, Ho, Er),^[21] RECo_{1–3}Sb₂ (RE = La–Nd, Sm, Gd),^[22–24] and α -type RECoSb₃ (RE = Ce, Pr).^[25,26]

In this paper, we present the syntheses and structures of a new series of β -type RECoSb₃ (RE = La–Nd, Sm). The structural relationship among parent type, α -, and β -type RE₂Sb₃ has been presented, and the electronic band structure calculations with the aid of the TB-LMTO method have been reported for the first time; also the electrical conductivity and the magnetic properties are investigated.

[a] State Key Laboratory of Structural Chemistry, Fujian Institute of Research on the Structure of Matter, Chinese Academy of Sciences, Fuzhou, Fujian 350002, People's Republic of China
Fax: +86-591-83704947
E-mail: chenl@fjirsm.ac.cn

[b] Graduate School of the Chinese Academy of Sciences, Beijing 100039, People's Republic of China

[c] State Key Laboratory for Physical Chemistry of Solid Surfaces, Xiamen University, Xiamen 361005, People's Republic of China

Results and Discussion

Structure

β - $RECoSb_3$ ($RE = La-Nd, Sm$) is the isostructural form of the β - $RENiSb_3$ -type compound.^[19] The anionic moiety of the structure consists of two independent parts: slightly distorted Sb square nets and $CoSb_6$ octahedron layers. Both are stacked along the a axis and separated by RE^{3+} cations as shown in Figure 1.

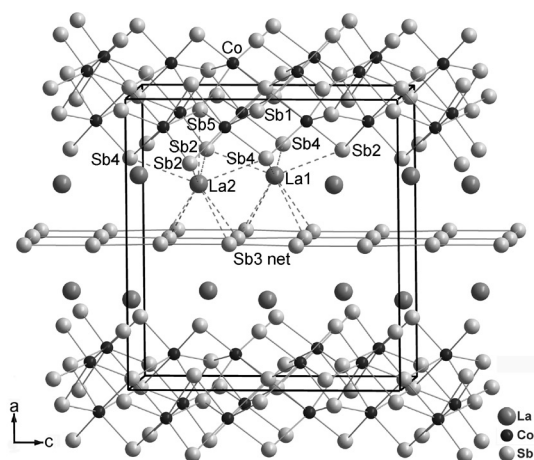


Figure 1. View down the b axis of β - $LaCoSb_3$ with the unit cell outlined. The coordination around the La1 and La2 atom is marked by dashed lines. For clarity, the Co–Co bonds are omitted.

To date, three structure types of antimonides with a common formula $RETSb_3$ ($T =$ transition metal), namely parent-type $RECrSb_3$,^[5] α -type $RENiSb_3$,^[17,18] and β -type $RENiSb_3$ ^[19] have been reported. Each structure has similar anionic building units, Sb square nets and TSb_6 octahedron layers, with RE^{3+} cations inserted between them. The major difference is their c parameters that are determined by the different building units along the c axis. As shown in Figure 2, in the parent-type $RECrSb_3$, the repeat unit is a monooctahedron $[CrSb_6]$ that extends along c through face-sharing. In the β -type, for example $LaCoSb_3$, the building unit is a dimer of the edge-shared octahedra, $[Co_2Sb_{10}]$. While in the α -type, for example $LaNiSb_3$, the building unit is a trimer of the edge-shared octahedra, $[Ni_3Sb_{14}]$. The dimer or trimer along c leads to the approximately doubled or tripled c -parameter for β - or α - $RETSb_3$, respectively. This relationship can also be understood by the stacking sequences of the close-packed layers of Sb atoms along the c direction as shown in Figure 2. Such stacking sequences are AB in parent- $LaCrSb_3$, ABCB in β - $LaCoSb_3$, and AB-ACBC in α - $LaNiSb_3$.

On the other hand, the connection motifs and repeat unit along the b axis are similar for the three types; therefore the b parameters are nearly the same, ranging from 6.160 Å for the β -type to 6.203 Å for the α -type and to 6.212 Å for the parent type.^[5,17] Meanwhile, the a -parameter is determined by the thickness of the TSb_6 octahedron layer, Sb square net, and the size of the interstitial RE^{3+} cations. Therefore, no significant change in a parameters is expected among

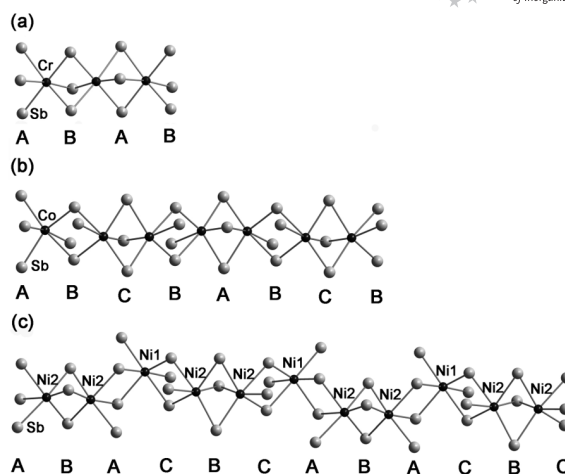


Figure 2. The connection motifs of the TSb_6 octahedra along the c axis of $RETSb_3$. (a): $T = Cr$, (b): $T = Co$, and (c): $T = Ni$. A, B, C represent the stacking sequences of the essentially close-packed Sb atoms.

the three types, for example 13.283 Å for parent-type $LaCrSb_3$ ^[5] and 12.985 Å for β -type $LaCoSb_3$, and 12.634 Å for α -type $CeNiSb_3$.^[17] The β -type $RECoSb_3$ has shown lanthanide contraction as indicated by Figure 3, in which the lattice parameters as well as the cell volumes decrease monotonically with the increase of the atomic number of the lanthanide.

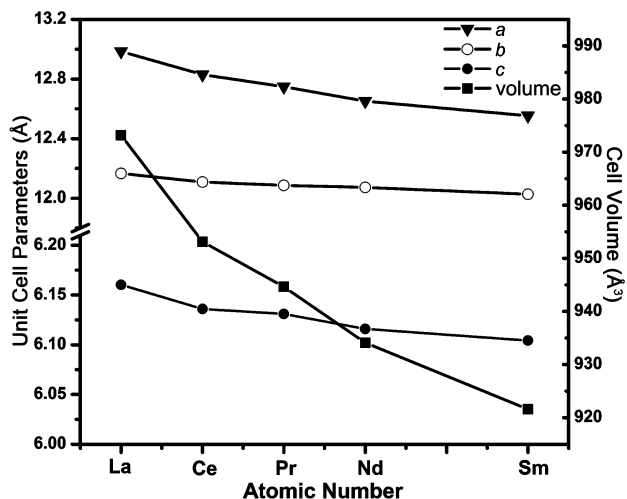


Figure 3. Plots of the lattice parameters [Å] and cell volumes [Å³] for β - $RECoSb_3$ ($RE = La-Nd, Sm$).

The five β - $RECoSb_3$ compounds reported here belong to the β -type structure. Taking $LaCoSb_3$ as an example, the Co–Sb bond lengths within the $CoSb_6$ octahedron range from 2.5918(13) Å to 2.6661(12) Å with an average (2.629 Å) similar to 2.588 Å in binary $CoSb$ (NiAs-type),^[27] but slightly longer than that in $CoSb_3$ (2.527 Å).^[28] The distortion of the TSb_6 octahedra is more obvious than that in parent-type $LaCrSb_3$,^[5] but comparable to that in $CoSb_3$.^[28] In addition, the Co–Co distances roughly decrease with a decrease in the size of RE^{3+} cations, 2.756(2) Å for La-, 2.735(2) Å for Ce-, 2.729(2) Å for Pr-, 2.739(2) Å for Nd-,

and 2.718(2) Å for the Sm-member. Such distances are slightly longer than 2.588 Å in binary CoSb.^[27] The Sb–Sb bonds in the Co/Sb layer, such as Sb1–Sb1 [3.1598(9) Å], Sb1–Sb4 [3.1426(14) Å], and Sb1–Sb5 [3.3410(1) Å], are longer than that in the Sb square net, for example Sb3–Sb3 [3.0128(12)–3.0806(9) Å].

There are two crystallographically independent La sites, La1 (Wyckoff site 4c) and La2 (4d) in β -LaCoSb₃. As depicted in Figure 4 (a), the La1 atom adopts a square antiprismatic coordination, which is frequently found in the rare-earth antimonides such as $RECo_{1-x}Sb_2$ ($RE = La, Ce, Pr, Nd, Sm, \text{ and } Gd$)^[22–24] or $RETSb_2$ ($T = Ag, Ga, Mn, Zn, Cd$).^[29–33] One square base is constructed by two Sb2 atoms and two Sb4 atoms from the Co/Sb layer, and the other is defined by four Sb3 atoms from the Sb net. The La2 atom has similar square antiprismatic geometry with an extra La2–Sb5 contact with the Co/Sb layer (Figure 4, b). Compared with the β -RENiSb₃ analogues, RE –Sb distances are not affected significantly by the different transition-metal ions, for example, 3.2573(9)–3.3940(9) Å for β -LaCoSb₃ and 3.2503(5)–3.3942(9) Å for β -LaNiSb₃.^[19] The square Sb nets are composed of Sb3 atoms with bond lengths of 3.0128(12)–3.0806(9) Å, and angle Sb–Sb–Sb: 87.434(5)–92.533(6)° as shown in Figure 5. Compared with the Ni-analogue, different transition metal, Co vs. Ni, slightly changes the bonds and angles. The Sb3 nets are

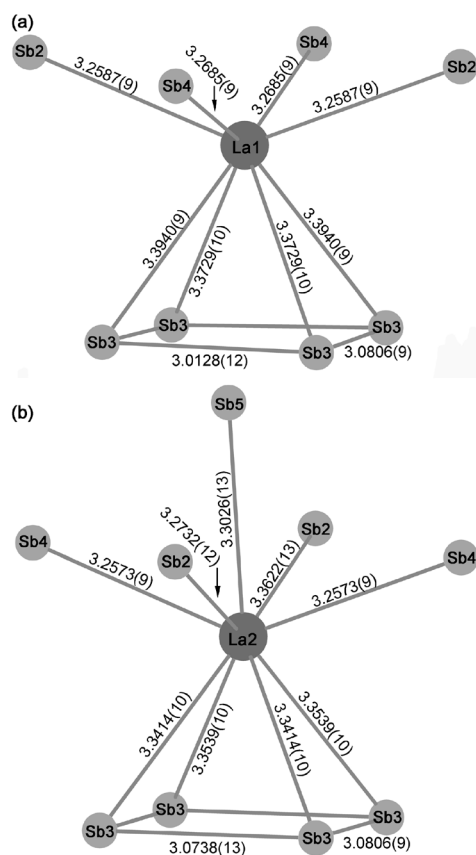


Figure 4. (a) La1 centered square antiprism. (b) La2 centered monocapped square antiprism. The La–Sb, and Sb3–Sb3 bond lengths less than 3.40 Å are indicated.

shown in Figure 5. The Sb nets in the parent type are an ideal square net with Sb–Sb: 3.049(5)–3.108(5) Å; angle Sb–Sb–Sb: 90°,^[5] and distorted in both α -type [3.0620(3)–3.1035(2) Å; 84.953(6)–94.944(6)°]^[17] and β -type [3.0084(7)–3.0702(8) Å; 88.236(19)–91.749(20)°].^[19] Such distortion is caused by the different connection motifs of the TSb₆ octahedra along the c direction as described above. On the other hand, different RE^{3+} cations barely influence the geometry, for example, in the series of β -RECoSb₃, from La to Sm, the shorter Sb3–Sb3 bond lengths change 1%, the longer Sb3–Sb3 bond lengths only change 0.9%, and the angular deviation is also negligible.

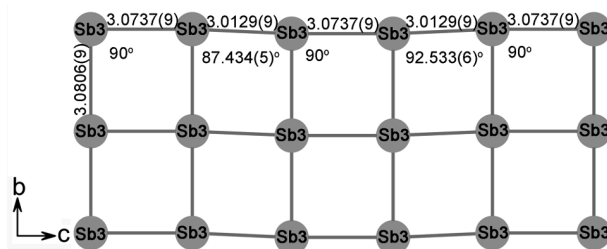


Figure 5. The Sb square nets in β -LaCoSb₃ in the bc -plane with angles and distances [Å] marked.

The structural comparison between β -RECoSb₃ and β -RENiSb₃ suggests that the different transition metal does not alter the crystallographic structure predominantly. The electronic structures have therefore been studied to give some insight into the physical properties.

Electronic Structure

The electronic structure for β -LaCoSb₃ was calculated with the TB-LMTO method. The band structure along the special symmetry lines Γ -X, Γ -Y, and Γ -Z is shown in Figure 6. Along Γ -Y, bands crossing the Fermi level are quite dispersed with contributions largely from the orbitals of either the Sb square net or Co/Sb layer extending along the b axis (Figure 7, parts a, b, d). The bands crossing the

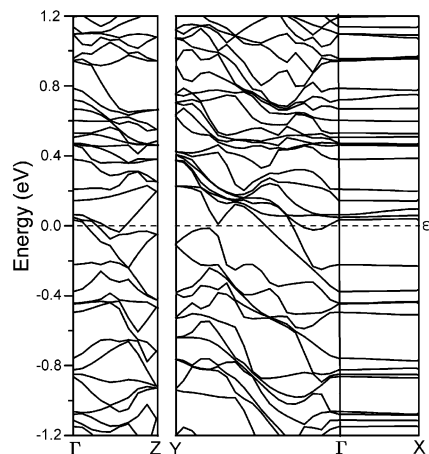


Figure 6. Band dispersion curves for β -LaCoSb₃ along Γ X, Γ Y, and Γ Z. The Fermi level ($\epsilon_f = 0$) is set to zero.

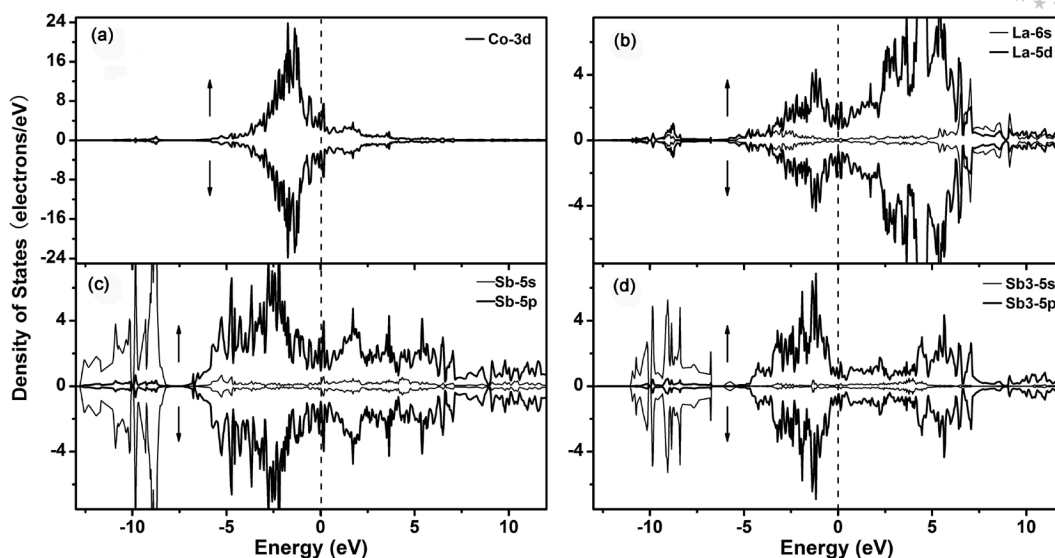


Figure 7. Spin-polarized densities of states (DOS) for β -LaCoSb₃. (a) Partial DOS of Co ions; (b) partial DOS of La cations; (c, d) partial DOS of Sb atoms from Co/Sb layer and Sb₃ atoms of Sb square net, respectively. The Fermi level is marked by a dashed line at 0 eV.

Fermi level along Γ -Z mainly correspond to the contributions of the layers of Co/Sb and Sb square net along the c axis. These features suggest that β -LaCoSb₃ should be metallic in both b and c directions. Meanwhile, the three types of RETSb₃ have similar electronic structures; therefore, their electronic properties should be comparable. This statement has been supported by the experimental measurements on β -LaNiSb₃ that displays metallic electrical conductivity from 1.8 K to 300 K along the b direction.^[19] And the parent-type LaCrSb₃ also exhibits metallic electrical conductivity from 20 K to 300 K along the c direction.^[7] As shown in Figure 6, the bands are flat along Γ -X and no band crosses the Fermi level, which is consistent with the existence of the intervening layers of La³⁺ ions that are weakly bonded to both the Sb net and Co/Sb layers. Therefore, RETSb₃ should show poor conductivity along the a axis. Such a prediction is worthy of further experimental measurement.

The spin-polarized calculations of the partial densities of states (DOS) of La, Co, and Sb atoms and the crystal orbital Hamilton population (COHP) curves for β -LaCoSb₃ are shown in Figure 7 and Figure 8. The Fermi level crosses partially filled bands in the DOS curve, which also indicates the metallic behavior. Most of the La states ($5d$ and $6s$) are unoccupied and locate above the Fermi level, as expected for an electropositive element. The hybridization of La $5d$ and Sb $5p$ states from -3 to 0 eV (Figure 7 b, c, d) implies some bonding character between La and Sb. For instance, La1-Sb bonds range from 3.2587(9) to 3.3940(9) Å, with the integrated $-COHP$ value varying from 1.017 to 0.837 eV/cell. Any La1-Sb bond longer than 3.50 Å is regarded as relatively weak because the integrated $-COHP$ value is only about half of the normal La1-Sb bonds. Similarly, the distances of La2-Sb bonds between 3.2573(9) and 3.3622(13) Å, with an average of 3.3098 Å are slightly

shorter, so the integrated $-COHP$ value of 0.909 eV/cell is larger than that of the La1 sphere. As shown in parts c and d of Figure 7, the partial DOS of Sb atoms in the Co/Sb layer are more delocalized than that of the square net, for example Sb $5p$ (-7 to 0 eV) vs. Sb₃ $5p$ (-4.5 to 0 eV), which illuminates that Sb atoms in the Co/Sb layer show abundant bonding interactions compared with that in the square net. In the region from -5 eV up to the Fermi level, a significant mixture of Co $3d$ and Sb $5p$ states implies the strong covalent character of Co-Sb bonds. As indicated by the COHP curves plotted in Figure 8 (b), the Co-Sb bonds (2.596–2.666 Å) within the CoSb₆ octahedra are almost optimized giving an integrated $-COHP$ value from 1.985 to 2.221 eV/cell. The Sb₃-Sb₃ bonds (3.0128–3.0806 Å) are covalent bonds with the integrated $-COHP$ value of 0.893–1.100 eV/cell. Any Sb-Sb distance beyond 3.3410 Å is not considered since the Sb1-Sb5 (3.3410 Å) only has an $-ICOHP$ about 12% of the strongest Sb₃-Sb₃ bond.

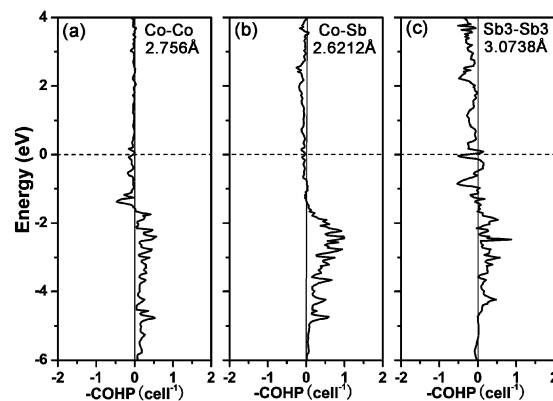


Figure 8. Crystal orbital Hamilton population curves for the Co-Co, Co-Sb, and Sb₃-Sb₃ in β -LaCoSb₃. The Fermi level is set at $\epsilon_F = 0$ eV.

The complex Sb substructure of β -LaCoSb₃ adds difficulty to charge formulation. A simple charge formulation would be La³⁺[CoSb₃]³⁻. The bond orders (v_{ij}) for the Sb atoms can be calculated by $v_{ij} = \exp[(2.80 - d_{ij})/0.37]$, where d_{ij} is the bond length in Å.^[35] The formal charges are thus calculated to be -1.9 for Sb1, -2.5 for Sb2, -1.0 for Sb3, -2.6 for Sb4, and -2.5 for Sb5, giving an overall negative charge of -5.75 per formula unit in β -LaCoSb₃. The calculated charge of Sb3 agrees well with that deduced from the Zintl-Klemm concept, i.e., four-bonded Sb3 atoms (Figure 5) in square nets is assigned to -1.^[2,34] This simple calculation reveals the apparent charge of Co as +2.75.

As shown in Figure 7 (a), the spin-up states (\uparrow) are almost the same as the spin-down states (\downarrow) around the Fermi level (the calculated magnetic moment is 0.000013 μ_B), indicating that β -LaCoSb₃ is not a spin-polarized compound. This also agrees with the diamagnetic behavior of Co atoms in many intermetallic compounds such as Ce₃Co₄Sn₁₃,^[36] RE₅Co₄Si₁₄ (RE = Ho, Er, Tm, Yb),^[37] RE₆Co_{1.67}Si₃ (RE = Ce, Nd, Gd, Tb, Dy).^[38] Our calculations allow us to make the statement that for the β -RETSb₃ series the rare-earth atoms are the only magnetic source. Such a statement has been substantiated by the isostructural β -CeNiSb₃ that shows an experimental effective magnetic moment close to the value for free Ce³⁺ cations.^[19] On the basis of these calculations and observations, the magnetism of β -RECoSb₃ should be identical to the corresponding Ni members. And the La members, β -LaCoSb₃ and β -LaNiSb₃, should be diamagnetic.

Conclusions

In summary, we have synthesized five new ternary β -type RECoSb₃ compounds with RE = La, Ce, Pr, Nd, and Sm.

The structure features the alternating layers of condensed CoSb₆ octahedra and square Sb nets, with interventional RE³⁺ cations. Electronic structure calculations on β -LaCoSb₃ show anisotropic metallic conductivities in both b and c directions that agree well with previous measurements. The conductivity in the a direction should be weak because of the intervention of RE³⁺ cations via weak bond interactions. The calculations also indicate no spin-polarization occurred around the Fermi level, which means that LaTSb₃ (T = Co, Ni) should be diamagnetic.^[19] And for other RE members, the magnetic rare-earth atoms are the only source for the magnetic properties. Therefore, the two series of β -type compounds, RECoSb₃ and RENiSb₃, should be identical in magnetism.

Experimental Section

Synthesis: The handling of all materials was carried out inside a N₂-filled glove box with controlled oxygen and moisture levels below 0.1 ppm. The rare-earth metals, La, Pr, Nd, and Sm (99.5% or higher, Huhhot Jinrui Rare Earth Co. Ltd), Ce foil (99.9%, Alfa Aesar), Co power (99.94%, Shanghai Guoyao group), Sb shot (99.999%, Alfa Aesar), and Sn shot (99.99%, Alfa Aesar) were used as received. Single crystals of β -RECoSb₃ (RE = La–Nd, Sm) were prepared with Sn flux. The stoichiometric elemental mixture of RE/Co/Sb (1:1:3 in molar ratio) and 0.3 g Sn was placed in an evacuated fused-silica tube, then flame-sealed under vacuum at 10⁻³ Pa. The sealed tubes were placed into a temperature-controlled tube furnace, heated at 640 °C for 1 d and 1050 °C for 3 d, and then cooled to room temperature over 8 d. The Sn flux was removed by hydrochloric acid, and the plate-like crystals were obtained after being washed with distilled water. These crystals were stable in air over a period of weeks.

The power samples were prepared with RE:Co:Sb (RE = La, Ce, Pr, Nd, and Sm) in 1:1:3.15 molar ratio (the excess of Sb was to

Table 1. Crystal data and structural refinements for β -RECoSb₃ (RE = La–Nd, Sm).

Chemical formula	LaCoSb ₃	CeCoSb ₃	PrCoSb ₃	NdCoSb ₃	SmCoSb ₃
Formula weight	563.09	564.30	565.09	568.42	574.57
Space group	<i>Pbcm</i> (No.57)	<i>Pbcm</i> (No.57)	<i>Pbcm</i> (No.57)	<i>Pbcm</i> (No.57)	<i>Pbcm</i> (No.57)
a [Å]	12.985(4)	12.829(8)	12.748(6)	12.651(5)	12.5530(13)
b [Å]	6.1603(18)	6.136(4)	6.131(3)	6.116(2)	6.1043(4)
c [Å]	12.166 (4)	12.109(7)	12.086(5)	12.073(4)	12.0267(12)
V [Å ³]	973.19(50)	953.14(10)	944.65(75)	934.13(57)	921.57(15)
Z	8	8	8	8	8
Crystal size [mm]	0.15/0.10/0.05	0.07/0.04/0.02	0.15/0.09/0.05	0.15/0.09/0.04	0.10/0.09/0.08
Temperature [K]	293(2)	293(2)	293(2)	293(2)	293(2)
ρ_{cal} [g/cm ³]	7.686	7.865	7.947	8.084	8.282
Radiation, λ [Å]	Mo-K α , 0.71073	Mo-K α , 0.71073			
θ range [°]	3.14–27.48	3.18–27.42	3.20–27.47	3.22–27.47	3.25–27.47
Index ranges	-16 $\leq h \leq$ 16 -7 $\leq k \leq$ 6 -14 $\leq l \leq$ 15	-16 $\leq h \leq$ 12 -7 $\leq k \leq$ 7 -15 $\leq l \leq$ 15	-16 $\leq h \leq$ 16 -7 $\leq k \leq$ 7 -13 $\leq l \leq$ 15	-14 $\leq h \leq$ 16 -7 $\leq k \leq$ 7 -15 $\leq l \leq$ 15	-16 $\leq h \leq$ 7 -7 $\leq k \leq$ 7 -15 $\leq l \leq$ 15
μ [mm ⁻¹]	28.171	29.351	30.293	31.319	33.221
R_{int}	0.0572	0.0375	0.0427	0.0643	0.0672
R_1/wR_2 [$I > 2\sigma(I)$] ^[a]	0.0316/0.0771	0.0232/0.0522	0.0256/0.0619	0.0457/0.1198	0.0326/0.0740
R_1/wR_2 (all data)	0.0355/0.0785	0.0275/0.0541	0.0279/0.0633	0.0463/0.1206	0.0385/0.0778
$\Delta\rho_{\text{max}}$ [e·Å ⁻³]	2.929	1.265	1.827	4.004	2.576
$\Delta\rho_{\text{min}}$ [e·Å ⁻³]	-3.329	-1.121	-1.951	-5.434	-2.349
Goodness of fit on F_o^2	1.094	1.092	1.158	1.184	1.094

[a] $R_1 = \sum |F_o| - |F_c| / \sum |F_o|$ for $F_o^2 > 2\sigma(F_o^2)$; $wR_2 = \sum [w(F_o^2 - F_c^2)] / \sum [w(F_o^2)^2]^{1/2}$, where $w = 1/[\sigma^2(F_o^2) + (AP)^2 + BP]$, and $P = (F_o^2 + 2F_c^2)/3$.

compensate for evaporative losses). The heating profile for each sample is 650 °C for 1 d and 950 °C for 8 d and then cooling to 300 °C at 5 °C/h before switching off the furnace. The X-ray diffraction analyses show the existence of the minor byproducts of CoSb_3 and CoSb_2 . With the purpose to obtain singular β - RE - CoSb_3 , the product was reground several times and pressed into a pellet, sealed in a silica tube, then heated at 900 °C for 8 d, and subsequently cooled to room temperature. Unfortunately, the byproducts, binary CoSb_3 and CoSb_2 (less than 10%), were irremovable by such treatment. The arc-melting technique yields β - RE - CoSb_3 as the major product together with minor CoSb_3 and CoSb_2 byproducts.

Similar reactions were carried out for other rare-earth metals with $RE = \text{Gd-Tm}$ and Y for proposed $RE\text{CoSb}_3$ analogs. However,

$RE\text{Co}_{1-x}\text{Sb}_2$ (HfCuSi_2 -type) with $RE = \text{Gd-Er}$ and Y were produced.^[39] When $RE = \text{Tm}$, binary TmSb was the main product.

In the diagram study of the $RE/\text{Co}/\text{Sb}$ ($RE = \text{Ce, Pr}$) system, two α -type compounds have been identified by XRD patterns, and their annealed temperatures are 400 °C and 600 °C, respectively.^[25,26] Therefore, β - $RE\text{CoSb}_3$ is thought to be a high-temperature stable phase.

Elemental Analysis: Microprobe elemental analysis was performed on some single crystals of $RE\text{CoSb}_3$, including the single crystals used for X-ray diffraction analyses. Spectra were collected on a field emission scanning electron microscope (FESEM, JSM6700F) equipped with an energy dispersive X-ray spectroscopy (EDX, Oxford INCA). The results indicated the presence of all three RE , Co ,

Table 2. Atomic positions, site symmetry, and U_{eq} values for β - $RE\text{CoSb}_3$ ($RE = \text{La-Nd, Sm}$).

Atom	Wyckoff site	x	y	z	$U_{eq} [\text{Å}^2]^{\text{[a]}}$
LaCoSb₃					
La1	4c	0.70093(5)	1/4	0	0.00514(18)
La2	4d	0.30412(5)	0.27003(11)	3/4	0.00490(18)
Co1	8e	0.09764(8)	0.03739(17)	0.86327(7)	0.00630(2)
Sb1	4c	0.97285(5)	1/4	0	0.00630(2)
Sb2	4d	0.79080(5)	0.26224(12)	3/4	0.00590(2)
Sb3	8e	0.50200(3)	0.51089(8)	0.87632(3)	0.00622(18)
Sb4	4c	0.21487(6)	1/4	0	0.00580(2)
Sb5	4d	0.94380(5)	0.88966(12)	3/4	0.00640(2)
CeCoSb₃					
Ce1	4c	0.70037(4)	1/4	0	0.00566(13)
Ce2	4d	0.30463(4)	0.26810(7)	3/4	0.00561(13)
Co1	8e	0.10094(7)	0.03510(13)	0.86292(6)	0.00853(19)
Sb1	4c	0.97276(5)	1/4	0	0.00790(15)
Sb2	4d	0.78711(4)	0.25898(8)	3/4	0.00624(14)
Sb3	8e	0.50195(3)	0.50995(6)	0.87627(3)	0.00675(12)
Sb4	4c	0.21779(5)	1/4	0	0.00628(14)
Sb5	4d	0.94424(4)	0.88655(9)	3/4	0.00780(15)
PrCoSb₃					
Pr1	4c	0.70016(4)	1/4	0	0.00526(15)
Pr2	4d	0.30507(4)	0.26982(8)	3/4	0.00529(14)
Co1	8e	0.10118(7)	0.03578(14)	0.86290(6)	0.00680(2)
Sb1	4c	0.97269(5)	1/4	0	0.00678(16)
Sb2	4d	0.78561(5)	0.25959(9)	3/4	0.00568(16)
Sb3	8e	0.50209(3)	0.51054(6)	0.87628(3)	0.00616(15)
Sb4	4c	0.21956(5)	1/4	0	0.00575(16)
Sb5	4d	0.94333(4)	0.88860(9)	3/4	0.00701(16)
NdCoSb₃					
Nd1	4c	0.70015(6)	1/4	0	0.00640(3)
Nd2	4d	0.30479(6)	0.27282(11)	3/4	0.00620(3)
Co1	8e	0.10065(9)	0.0376(2)	0.86343(9)	0.00850(3)
Sb1	4c	0.97244(7)	1/4	0	0.00760(3)
Sb2	4d	0.78390(7)	0.26240(12)	3/4	0.00660(3)
Sb3	8e	0.50246(4)	0.51204(10)	0.87615(4)	0.00710(3)
Sb4	4c	0.22162(8)	1/4	0	0.00690(3)
Sb5	4d	0.94260(6)	0.89053(12)	3/4	0.00740(3)
SmCoSb₃					
Sm1	4c	0.69968(6)	1/4	0	0.00685(18)
Sm2	4d	0.30568(6)	0.27138(9)	3/4	0.00681(18)
Co1	8e	0.10342(11)	0.03549(18)	0.86301(9)	0.01070(3)
Sb1	4c	0.97241(8)	1/4	0	0.00890(2)
Sb2	4d	0.78138(8)	0.25914(11)	3/4	0.00720(2)
Sb3	8e	0.50244(5)	0.51076(8)	0.87615(4)	0.00769(19)
Sb4	4c	0.22393(8)	1/4	0	0.00730(2)
Sb5	4d	0.94300(7)	0.88831(12)	3/4	0.00900(2)

[a] U_{eq} is defined as one-third of the trace of the orthogonalized U_{ij} tensor.

Table 3. Selected interatomic distances [\AA] in $\beta\text{-RECoSb}_3$ ($RE = \text{La-Nd, Sm}$).

	LaCoSb ₃	CeCoSb ₃	PrCoSb ₃	NdCoSb ₃	SmCoSb ₃
RE1-Sb1	3.5308(14)	3.4950(2)	3.4743(18)	3.4447(17)	3.4237(12)
RE1-Sb2 ($\times 2$)	3.2587(9)	3.2258(18)	3.2125(13)	3.1997(10)	3.1773(5)
RE1-Sb3 ($\times 2$)	3.3729(10)	3.3392(14)	3.3226(12)	3.3052(11)	3.2846(8)
RE1-Sb3 ($\times 2$)	3.3940(9)	3.3568(14)	3.3412(11)	3.3256(11)	3.2988(8)
RE1-Sb4 ($\times 2$)	3.2685(9)	3.2425(18)	3.2317(14)	3.2141(10)	3.1992(4)
RE2-Co1	3.3379(13)	3.2774(16)	3.2676(14)	3.2581(15)	3.2198(14)
RE2-Sb2	3.2732(12)	3.2337(19)	3.2175(15)	3.1975(13)	3.1717(9)
RE2-Sb2	3.3622(13)	3.3381(19)	3.3349(15)	3.3173(14)	3.3124(9)
RE2-Sb3 ($\times 2$)	3.3414(10)	3.3087(14)	3.2887(12)	3.2732(11)	3.2462(8)
RE2-Sb3 ($\times 2$)	3.3539(10)	3.3172(14)	3.3015(11)	3.2879(11)	3.2610(8)
RE2-Sb4 ($\times 2$)	3.2573(9)	3.2277(18)	3.2146(13)	3.1994(10)	3.1797(5)
RE2-Sb5	3.3026(13)	3.2740(2)	3.2494(16)	3.2115(16)	3.2023(12)
Co1-Co1	2.756(2)	2.735(2)	2.7291(19)	2.739(2)	2.718(2)
Co1-Sb1 ($\times 2$)	2.5960(12)	2.5902(13)	2.5889(11)	2.5820(14)	2.5802(12)
Co1-Sb1($\times 2$)	2.6661(12)	2.6829(13)	2.6747(11)	2.6528(14)	2.6708(13)
Co1-Sb2($\times 2$)	2.6212(13)	2.6081(13)	2.6100(12)	2.6155(15)	2.6047(13)
Co1-Sb4	2.6076(12)	2.5963(13)	2.5977(11)	2.5979(14)	2.5919(13)
Co1-Sb5	2.5918(13)	2.5965(14)	2.5934(13)	2.5849(15)	2.5903(15)
Co1-Sb5	2.6265(14)	2.6183(15)	2.6197(13)	2.6144(15)	2.6125(13)
Sb1-Sb1 ($\times 2$)	3.1598(9)	3.1464(19)	3.1435(14)	3.1365(10)	3.1297(5)
Sb1-Sb4	3.1426(14)	3.1430(2)	3.1472(17)	3.1525(18)	3.1574(14)
Sb1-Sb5 ($\times 2$)	3.3410(1)	3.3166(17)	3.3164(13)	3.3172(10)	3.2985(5)
Sb2-Sb5	3.0356(12)	3.0472(15)	3.0358(13)	3.0338(14)	3.0398(12)
Sb3-Sb3	3.0128(12)	2.9994(19)	2.9940(15)	2.9947(14)	2.9825(10)
Sb3-Sb3	3.0738(13)	3.0580(2)	3.0526(15)	3.0460(14)	3.0344(10)
Sb3-Sb3 ($\times 2$)	3.0806(9)	3.0682(19)	3.0658(14)	3.0586(10)	3.0528(2)

and Sb elements in molar ratios (19–21% RE, 19–20% Co, 58–62% Sb) and no Sn element was detected, which is in good agreement with the stoichiometry refined from the single-crystal X-ray structure determinations.

Structure Determination: The single-crystal X-ray diffraction data were collected with a Rigaku Mercury CCD diffractometer equipped with a graphite-monochromated Mo- K_α radiation source ($\lambda = 0.71073 \text{ \AA}$) at 293 K. The absorption corrections were done by the Multi-scan method.^[40] The space group was determined to be *Pbcm* (No. 57) based on systematic absences, E-value statistics, and subsequent successful refinements of the crystal structure. The structures were solved without events by direct methods and refined by full-matrix least-squares fitting on F^2 by SHELXL-97.^[41] All of the atoms were refined with anisotropic thermal parameters. Crystallographic data and structural refinements are summarized in Table 1. Atomic coordinates and anisotropic displacement parameters are provided in Table 2. Table 3 gives the interatomic distances for $\beta\text{-RECoSb}_3$ ($RE = \text{La-Nd, Sm}$) for comparison.

Further data, in the form of a crystallographic information file (CIF) can be obtained from the Fachinformationszentrum Karlsruhe, Abt. PROKA, 76344 Eggenstein-Leopoldshafen, Germany (Fax: +49-7247-808-666; E-mail: crysdata@fiz.karlsruhe.de) on quoting the depository numbers: CSD-419540 (for LaCoSb₃), CSD-419539 (for CeCoSb₃), CSD-419542 (for PrCoSb₃), CSD-419541 (for NdCoSb₃), and CSD-419538 (for SmCoSb₃).

Electronic Structure Calculations: The electronic structure calculations for $\beta\text{-LaCoSb}_3$ were performed by the linear muffin-tin orbital method^[42] with the aid of the TB-LMTO program.^[43] Exchange and correlation were treated in the local density approximation (LDA).^[44] The basis set included the 4*f*, 5*d*, 6*s*, 6*p* orbitals for La, 3*d*, 4*s*, 4*p* orbitals for Co, and 4*f*, 5*s*, 5*p*, 5*d* orbitals for Sb. The La 6*p*, Co 4*p*, and Sb 4*f*, 5*d* orbitals were treated with the downfolding technique.^[45] The *k*-space integrations were performed

by the tetrahedron method^[46] using a $2 \times 2 \times 4$ *k*-mesh within the Brillouin zone. The Fermi level ($\epsilon_f = 0 \text{ eV}$) was selected as the energy reference.

Acknowledgments

The research was supported by the National Natural Science Foundation of China under Projects (20521101, 20773130, 20733003), “Key Project from Fujian Institute of Research on the Structure of Matter” (SZD08002), and the “Key Project from Chinese Academy of Sciences” (KJCX2-YW-H01).

- [1] A. M. Mills, R. Lam, M. J. Ferguson, L. Deakin, A. Mar, *Coord. Chem. Rev.* **2002**, 233–234, 207–222.
- [2] G. A. Papoian, R. Hoffmann, *Angew. Chem. Int. Ed.* **2000**, 39, 2408–2448.
- [3] S. M. Kauzlarich, *Chemistry, Structure and Bonding of Zintl Phases and Ions*, VCH Publishers, New York, **1996**.
- [4] A. S. Sefat, S. L. Bud'ko, P. C. Canfield, *J. Magn. Magn. Mater.* **2008**, 320, 120–141.
- [5] M. J. Ferguson, R. W. Hushagen, A. Mar, *J. Alloys Compd.* **1997**, 249, 191–198.
- [6] K. Hartjes, W. Jeitschko, M. Brylak, *J. Magn. Magn. Mater.* **1997**, 173, 109–116.
- [7] N. P. Raju, J. E. Greedan, M. J. Ferguson, A. Mar, *Chem. Mater.* **1998**, 10, 3630–3635.
- [8] L. Deakin, M. J. Ferguson, A. Mar, J. E. Greedan, A. S. Wills, *Chem. Mater.* **2001**, 13, 1407–1412.
- [9] L. Deakin, A. Mar, *Chem. Mater.* **2003**, 15, 3343–3346.
- [10] S. J. Crerar, L. Deakin, A. Mar, *Chem. Mater.* **2005**, 17, 2780–2784.
- [11] E. L. Thomas, D. P. Gautreaux, J. Y. Chan, *Acta Crystallogr., Sect. E* **2006**, 62, i96–i98.

- [12] A. Thamizhavel, H. Nakashima, T. Shiromoto, Y. Obiraki, T. D. Matsuda, Y. Haga, S. Ramakrishnan, T. Takeuchi, R. Settai, Y. Ōnuki, *J. Phys. Soc. Jpn.* **2005**, *74*, 2617–2621.
- [13] M. Brylak, W. Jeitschko, *Z. Naturforsch. B: Chem. Sci.* **1995**, *50*, 899.
- [14] M. Leonard, S. Saha, N. Ali, *J. Appl. Phys.* **1999**, *85*, 4759–4761.
- [15] M. L. Leonard, I. S. Dubenko, N. Ali, *J. Alloys Compd.* **2000**, *303–304*, 265–269.
- [16] D. D. Jackson, Z. Fisk, *J. Magn. Magn. Mater.* **2003**, *256*, 106–116.
- [17] R. T. Macaluso, D. M. Wells, R. E. Sykora, T. E. Albrecht-Schmitt, A. Mar, S. Nakatsuji, H. Lee, Z. Fisk, J. Y. Chan, *J. Solid State Chem.* **2004**, *177*, 293–298.
- [18] E. L. Thomas, R. T. Macaluso, H.-O. Lee, Z. Fisk, J. Y. Chan, *J. Solid State Chem.* **2004**, *177*, 4228–4236.
- [19] E. L. Thomas, D. P. Gautreaux, H. O. Lee, Z. Fisk, J. Y. Chan, *Inorg. Chem.* **2007**, *46*, 3010–3016.
- [20] D. P. Gautreaux, C. Capan, J. F. DiTusa, D. P. Young, J. Y. Chan, *J. Solid State Chem.* **2008**, *181*, 1977–1982.
- [21] Y. Verbovytsky, K. Latka, *J. Alloys Compd.* **2008**, *450*, 272–275.
- [22] A. Leithe-Jasper, P. Rogl, *J. Alloys Compd.* **1994**, *203*, 133–136.
- [23] L.-M. Zeng, S.-W. Wu, W. Qin, *Trans. Nonferrous Met. Soc. China* **1997**, *7*, 60–62.
- [24] G. Cordier, H. Schaefer, P. Woll, *Z. Naturforsch., Teil B* **1985**, *40*, 1097–1099.
- [25] R. M. Luo, F. S. Liu, J. Q. Li, X. W. Feng, *J. Alloys Compd.*, DOI:10.1016/j.jallcom.2008.03.061.
- [26] S. Chykhrij, V. B. Smetana, *Inorg. Mater.* **2006**, *42*, 503–507.
- [27] T. Chen, J. C. Mikkelsen, G. B. Charlan, *J. Cryst. Growth* **1978**, *43*, 5–12.
- [28] T. Schmidt, G. Kliche, H. D. Lutz, *Acta Crystallogr., Sect. C* **1987**, *43*, 1678–1679.
- [29] O. Sologub, K. Hiebl, P. Rogl, O. Bodak, *J. Alloys Compd.* **1995**, *227*, 40–43.
- [30] L. Zeng, X. Xie, H. F. Franzen, *J. Alloys Compd.* **2002**, *343*, 122–124.
- [31] O. Sologub, H. Noel, A. Leithe-Jasper, P. Rogl, O. I. Bodak, *J. Solid State Chem.* **1995**, *115*, 441–446.
- [32] H. Flandorfer, O. Sologub, C. Godart, K. Hiebl, A. Leithe-Jasper, P. Rogl, H. Noel, *Solid State Commun.* **1996**, *97*, 561–565.
- [33] R. Wang, H. Steinfink, *Inorg. Chem.* **1967**, *6*, 1685–1692.
- [34] E. Zintl, *Angew. Chem.* **1939**, *52*, 1–6.
- [35] W. Jeitschko, R. O. Altmeyer, M. Schelk, U. C. Rodewald, *Z. Anorg. Allg. Chem.* **2001**, *627*, 1932–1940.
- [36] E. Lyle Thomas, H.-O. Lee, A. N. Bankston, S. MaQuilon, P. Klavins, M. Moldovan, D. P. Young, Z. Fisk, J. Y. Chan, *J. Solid State Chem.* **2006**, *179*, 1642–1649.
- [37] J. R. Salvador, C. Malliakas, J. R. Gour, M. G. Kanatzidis, *Chem. Mater.* **2005**, *17*, 1636–1645.
- [38] B. Chevalier, E. Gaudin, F. Weill, *J. Alloys Compd.* **2007**, *442*, 149–151.
- [39] W.-Z. Cai, L. Chen, unpublished results.
- [40] R. Corp, *CrystalClear*, version 1.3.5, Woodlands, Texas (USA), **1999**.
- [41] G. M. Sheldrick, *SHELXL-97: Program for Crystal Structure Solution*, University of Göttingen, Göttingen (Germany), **1997**.
- [42] a) O. K. Andersen, *Phys. Rev. B* **1975**, *12*, 3060–3083; b) H. L. Skriver, *The LMTO Method*, Springer, Berlin (Germany), **1984**.
- [43] O. Jepsen, O. K. Andersen, *The Stuttgart TB-LMTO Program, Version 4.7*, Max-Planck-Institut für Festkörperforschung, Stuttgart (Germany).
- [44] U. von Barth, L. Hedin, *J. Phys. C* **1972**, *5*, 1629–1642.
- [45] W. R. L. Lambrecht, O. K. Andersen, *Phys. Rev. B* **1986**, *34*, 2439–2449.
- [46] P. E. Blöchl, O. Jepsen, O. K. Andersen, *Phys. Rev. B* **1994**, *49*, 16223–16233.

Received: August 21, 2008

Published Online: December 9, 2008